Table 4. Overview of nucleotide 1896, 1762, and 1764 sequencing data with the deep sequencing analyses.

Case	G1896A		A1762T		G1764A	
	Base counts	(%)	Base counts	(%)	Base counts	(%)
Reactivation from occult HBV carrier status						
#1	1/10,833	(0.0)	0/6391	(0.0)	1/6491	(0.0)
#2	1/10,200	(0.0)	0/9213	(0.0)	3/9216	(0.0)
#3	8/27,694	(0.0)	1/16,506	(0.0)	4/16,851	(0.0)
#4	4/13,008	(0.0)	2/12,007	(0.0)	0/11,857	(0.0)
#5	0/6860	(0.0)	0/6175	(0.0)	0/6307	(0.0)
#6	273/31,622	(0.9)	8/29,996	(0.0)	4/30,400	(0.0)
#7	22/12,561	(0.2)	0/3405	(0.0)	1/3492	(0.0)
#8	1/11,500	(0.0)	0/4964	(0.0)	1/5089	(0.0)
#9	12,897/12,904	(100)	11,676/11,677	(100)	11,653/11,659	(100)
#10	11,432/11,444	(100)	1/6153	(0.0)	2/6217	(0.0)
#11	9533/9539	(99.9)	7669/7671	(100)	7681/7685	(99.9)
#12	10,944/10,945	(100)	2/10,874	(0.0)	1/11,325	(0.0)
#13*	9358/9411	(99.4)	2/10,900	(0.0)	0/11,298	(0.0)
#14*	11,174/11,179	(100)	0/6579	(0.0)	2/6773	(0.0)
Reactivation from HBsAg carrier status						
#15	734/12,544	(5.9)	7593/7596	(100)	7556/7570	(99.8)
#16	2/7469	(0.0)	0/6481	(0.0)	2/6618	(0.0)
#17	12,251/12,701	(96.5)	5110/5241	(97.5)	5180/5239	(98.9)
#18	9649/9660	(99.9)	0/10,026	(0.0)	0/10,069	(0.0)
#19	18,402/18,413	(99.9)	1/15,677	(0.0)	3/16,045	(0.0)
#20*	11,158/11,160	(100)	0/6671	(0.0)	3/6929	(0.0)

*Patients who developed fatal acute liver failure.

malignancy, we observed two patients without hematological malignancies who developed HBV reactivation. One case had colon cancer, with S-1 treatment triggering HBV exacerbation. Another case had psoriasis and received cyclosporine before the onset of HBV reactivation. Previously, we also reported a case of lethal *de novo* HBV hepatitis induced by adalimumab treatment for rheumatoid arthritis [26]. Thus, it is important to note that there is a risk of HBV reactivation in patients not only with hematological malignancies but also with solid tumors or non-cancerous diseases undergoing chemotherapy or immunosuppressive therapy. In addition, it is very important to regularly monitor HBV DNA levels to achieve the early administration of ETV before the onset of ALT elevation; however, the optimum frequency of HBV DNA testing in occult HBV carriers is not yet defined. A recent prospective study suggested that monthly monitoring of HBV DNA levels for lymphoma patients with resolved HBV infection might be a reasonable option during and after rituximab-CHOP chemotherapy [27].

To clarify the virological characteristics of HBV reactivation, we determined the genetic heterogeneity of viruses from patient sera. We found that the genetic complexity of the reactivated viruses in 14 patients with reactivation from occult HBV infection was significantly lower than that in six patients with reactivation from HBsAg carriers. There was no significant difference in circulating HBV DNA levels in serum after reactivation in both groups. The viral population in the sera of patients with reactivation from occult HBV infection was characterized by low heterogeneity, with nearly monoclonal viruses detected. We further examined the genetic complexity of latently infected HBV in the liver of 44 individuals with occult HBV infection. We found that the genetic heterogeneity of latently infected viruses in their livers was also very low. In one case we confirmed that the viral genome detected in serum after viral reactivation was almost identical to that in the latently infected liver before reactivation. These findings possibly suggest that the viral population in latently infected livers of occult HBV carriers is characterized by low heterogeneity, and the predominant viral clone increases in number under immunosuppressive conditions. The reason for the difference in the degree of genetic heterogeneity in the exacerbated viruses between patients with reactivation from occult infection and those with HBsAg carrier reactivation is unclear. One possibility is that the low levels of viral heterogeneity observed in occult HBV carriers are due to the relatively lower levels of viral replication compared with those of HBsAg carriers. Pollicino *et al.* demonstrated that the host immune system, not viral factors, likely plays a critical role in the strong suppression of viral replication and gene expression [28]. Since we could confirm the genetic homology of HBV DNA in the liver before reactivation and the serum after reactivation in only one case, further studies are required to determine the characteristics of the latent viruses in HBsAg-negative but anti-HBc-positive occult HBV carriers.

In this study, we found that 42.9% of cases that experienced HBV reactivation predominantly contained the G1896A pre-C variant in their sera. Infection with the G1896A variant was predominant in the liver of 11.4% of individuals with occult HBV infection. Patients acutely infected with the HBV G1896A pre-C variant have a high risk of developing ALF [16–18]. The G1896A variant is frequently detected in reactivated viruses in patients with reactivation from occult HBV infection that develop ALF [20]. We revealed that both patients who developed fatal ALF predominantly contained G1896A pre-C variants. The mechanism by which the G1896A mutation triggers the development of ALF

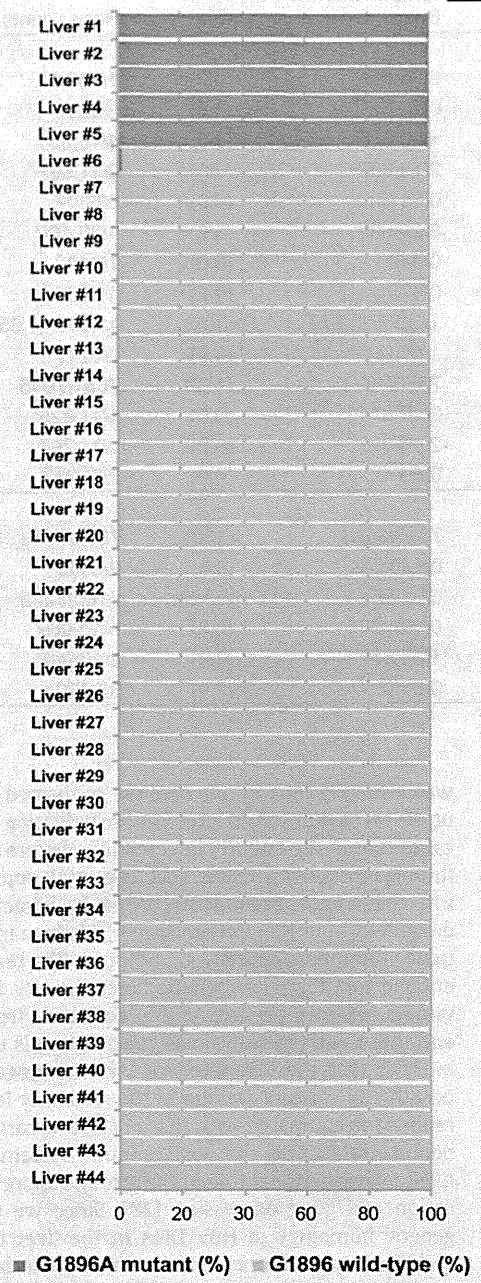

	Ratio of G1896A mutant (%)	Number of G1896A mutant/total nucleotides
Liver #1	100	61,007/61,007
Liver #2	100	37,772/37,772
Liver #3	100	28,522/28,522
Liver #4	100	31,058/31,058
Liver #5	100	22,305/22,306
Liver #6	1.65	603/36,540
Liver #7	0.04	25/65,560
Liver #8	0.01	4/34,524
Liver #9	0	0/6250
Liver #10	0	0/3713
Liver #11	0	0/28,607
Liver #12	0	0/19,565
Liver #13	0	0/30,432
Liver #14	0	0/25,118
Liver #15	0	0/44,475
Liver #16	0	0/18,628
Liver #17	0	0/56,581
Liver #18	0	0/33,525
Liver #19	0	0/65,535
Liver #20	0	0/27,574
Liver #21	0	0/38,029
Liver #22	0	0/28,124
Liver #23	0	0/34,889
Liver #24	0	0/38,163
Liver #25	0	0/22,696
Liver #26	0	0/41,092
Liver #27	0	0/35,525
Liver #28	0	0/27,640
Liver #29	0	0/48,424
Liver #30	0	0/27,096
Liver #31	0	0/35,044
Liver #32	0	0/45,925
Liver #33	0	0/55,458
Liver #34	0	0/28,405
Liver #35	0	0/40,664
Liver #36	0	0/65,535
Liver #37	0	0/32,852
Liver #38	0	0/39,434
Liver #39	0	0/28,938
Liver #40	0	0/16,115
Liver #41	0	0/19,120
Liver #42	0	0/49,353
Liver #43	0	0/37,564
Liver #44	0	0/24,832

Fig. 3. Prevalence of G1896A pre-core mutants in the liver of 44 healthy occult HBV carriers. The ratio of G1896A mutants to wild-type G1896 for total reads is shown in the left panel. The number of G1896A mutants, total reads at nucleotide position 1896, and the proportion of G1896A mutants (%) are shown in the right panel. (This figure appears in colour on the web.)

remains unknown at present. Previous studies reported that the G1896A variant has increased replication activity compared with the wild-type strain in vitro [18,29], but we found no significant association between the levels of circulating HBV DNA and the ratios of wild-type/G1896A pre-C mutants in cases with reactivation from occult HBV infection. On the other hand, it is well recognized that HBeAg/anti-HBe serostatus is closely associated with the ratios of wild-type/G1896A pre-C mutants in patients with chronic HBV infection [30]. Interestingly, accumulating evidence suggests that G1896A mutations abrogating HBeAg synthesis remove the tolerogenic effect of HBeAg, leading to an enhanced immune response that contributes to ALF development [31]. We must also pay attention to the genotype of HBV in cases with viral reactivation. Among the 14 cases with reactivation from occult HBV infection, genotype B and C strains were detected in five and nine patients, respectively. Among them, three of five cases were negative for HBeAg but positive for anti-HBe (60%) in genotype B and three of nine (33.3%) were genotype C-infected patients, and both cases with developing ALF were negative for HBeAg and infected with genotype B.

Previous studies demonstrated that HBV genotypes affect the liver disease outcome [32], and genotype B strain is frequently detected in patients developing ALF [18]. Thus, it is possible that the ratios of wild-type/G1896A pre-C mutants and viral genotype influence the pathophysiology of viral reactivation.

In conclusion, our findings suggest that HBV reactivation can occur during and after termination of chemotherapy or immunosuppressive therapy in occult HBV carriers with underlying hematological malignancies, solid tumors or non-cancerous diseases. Occult HBV infection and the resulting HBV reactivation is characterized by low genetic heterogeneity. It is unclear whether occult HBV carriers with the G1896A pre-C variant have an increased risk of developing HBV reactivation and fatal ALF. Further analysis with a larger cohort of patients is required to clarify the frequency and mechanisms of HBV reactivation and ALF in patients with occult HBV carrier status receiving chemotherapy or immunosuppressive therapy.

Financial support

This work was supported by Japan Society for the Promotion of Science (JSPS) Grants-in-aid for Scientific Research, Health and Labour Sciences Research Grants for Research on Intractable Diseases, hepatitis, and Research on Hepatitis from the Ministry of Health, Labour and Welfare, Japan.

Conflict of interest

The authors who have taken part in this study declared that they do not have anything to disclose regarding funding or conflict of interest with respect to this manuscript.

Authors' contribution

Conceived and designed the experiments: TI, HM. Performed the experiments: TI, HM, HM. Analyzed the data: TI, YF, HM. Contributed reagents/materials/analysis tools: TI, YU, MU, TK, YO, SU, HM, TC. Wrote the paper: TI, YU, HM, TC.

Acknowledgments

We thank Dr. K. Takahashi, Dr. N. Nishijima, Dr. T. Shimizu, Mrs. K. Fujii, Dr. A. Sekine, Mr. T. Kitamoto, and Mrs. A. Kitamoto for ultra-deep sequencing analysis.

Supplementary data

Supplementary data associated with this article can be found, in the online version, at http://dx.doi.org/10.1016/j.jhep.2014.04.033.

References

[1] Wands JR, Chura CM, Roll FJ, Maddrey WC. Serial studies of hepatitis-associated antigen and antibody in patients receiving antitumor chemotherapy for myeloproliferative and lymphoproliferative disorders. Gastroenterology 1975;68:105–112.
[2] Galbraith RM, Eddleston AL, Williams R, Zuckerman AJ. Fulminant hepatic failure in leukaemia and choriocarcinoma related to withdrawal of cytotoxic drug therapy. Lancet 1975;2:528–530.
[3] Hoofnagle JH, Dusheiko GM, Schafer DF, Jones EA, Micetich KC, Young RC, et al. Reactivation of chronic hepatitis B virus infection by cancer chemotherapy. Ann Intern Med 1982;96:447–449.
[4] Lok AS, Liang RH, Chiu EK, Wong KL, Chan TK, Todd D. Reactivation of hepatitis B virus replication in patients receiving cytotoxic therapy. Report of a prospective study. Gastroenterology 1991;100:182–188.
[5] Dervite I, Hober D, Morel P. Acute hepatitis B in a patient with antibodies to hepatitis B surface antigen who was receiving rituximab. N Engl J Med 2001;344:68–69.
[6] Hui CK, Cheung WW, Zhang HY, Au WY, Yueng YH, Leung AY, et al. Kinetics and risk of de novo hepatitis B infection in HBsAg-negative patients undergoing cytotoxic chemotherapy. Gastroenterology 2006;131:59–68.
[7] Mason AL, Xu L, Guo L, Kuhns M, Perrillo RP. Molecular basis for persistent hepatitis B virus infection in the liver after clearance of serum hepatitis B surface antigen. Hepatology 1998;27:1736–1742.
[8] Raimondo G, Allain JP, Brunetto MR, Buendia MA, Chen DS, Colombo M, et al. Statements from the Taormina expert meeting on occult hepatitis B virus infection. J Hepatol 2008;49:652–657.
[9] Uemoto S, Sugiyama K, Marusawa H, Inomata Y, Asonuma K, Egawa H, et al. Transmission of hepatitis B virus from hepatitis B core antibody-positive donors in living related liver transplants. Transplantation 1998;65:494–499.
[10] Marusawa H, Uemoto S, Hijikata M, Ueda Y, Tanaka K, Shimotohno K, et al. Latent hepatitis B virus infection in healthy individuals with antibodies to hepatitis B core antigen. Hepatology 2000;31:488–495.
[11] Marusawa H, Imoto S, Ueda Y, Chiba T. Reactivation of latently infected hepatitis B virus in a leukemia patient with antibodies to hepatitis B core antigen. J Gastroenterol 2001;36:633–636.
[12] Lok AS, McMahon BJ. Chronic hepatitis B. Hepatology 2007;45:507–539.
[13] Kusumoto S, Tanaka Y, Mizokami M, Ueda R. Reactivation of hepatitis B virus following systemic chemotherapy for malignant lymphoma. Int J Hematol 2009;90:13–23.
[14] Rodriguez C, Chevaliez S, Bensadoun P, Pawlotsky JM. Characterization of the dynamics of hepatitis B virus resistance to adefovir by ultra-deep pyrosequencing. Hepatology 2013;58:890–901.
[15] Nishijima N, Marusawa H, Ueda Y, Takahashi K, Nasu A, Osaki Y, et al. Dynamics of hepatitis B virus quasispecies in association with nucleos(t)ide analogue treatment determined by ultra-deep sequencing. PLoS One 2012;7:e35052.
[16] Omata M, Ehata T, Yokosuka O, Hosoda K, Ohto M. Mutations in the precore region of hepatitis B virus DNA in patients with fulminant and severe hepatitis. N Engl J Med 1991;324:1699–1704.
[17] Carman WF, Fagan EA, Hadziyannis S, Karayiannis P, Tassopoulos NC, Williams R, et al. Association of a precore genomic variant of hepatitis B virus with fulminant hepatitis. Hepatology 1991;14:219–222.
[18] Ozasa A, Tanaka Y, Orito E, Sugiyama M, Kang JH, Hige S, et al. Influence of genotypes and precore mutations on fulminant or chronic outcome of acute hepatitis B virus infection. Hepatology 2006;44:326–334.
[19] Steinberg JL, Yeo W, Zhong S, Chan JY, Tam JS, Chan PK, et al. Hepatitis B virus reactivation in patients undergoing cytotoxic chemotherapy for solid tumours: precore/core mutations may play an important role. J Med Virol 2000;60:249–255.
[20] Umemura T, Tanaka E, Kiyosawa K, Kumada H. Mortality secondary to fulminant hepatic failure in patients with prior resolution of hepatitis B virus infection in Japan. Clin Infect Dis 2008;47:e52–e56.
[21] Marusawa H, Osaki Y, Kimura T, Ito K, Yamashita Y, Eguchi T, et al. High prevalence of anti-hepatitis B virus serological markers in patients with hepatitis C virus related chronic liver disease in Japan. Gut 1999;45:284–288.
[22] Cholongitas E, Papatheodoridis GV, Burroughs AK. Liver grafts from anti-hepatitis B core positive donors: a systematic review. J Hepatol 2010;52:272–279.
[23] Chevaliez S, Rodriguez C, Pawlotsky JM. New virologic tools for management of chronic hepatitis B and C. Gastroenterology 2012;142:e1301.
[24] Polson J, Lee WM. AASLD position paper: the management of acute liver failure. Hepatology 2005;41:1179–1197.
[25] Sato S, Suzuki K, Akahane Y, Akamatsu K, Akiyama K, Yunomura K, et al. Hepatitis B virus strains with mutations in the core promoter in patients with fulminant hepatitis. Ann Intern Med 1995;122:241–248.
[26] Matsumoto T, Marusawa H, Dogaki M, Suginoshita Y, Inokuma T. Adalimumab-induced lethal hepatitis B virus reactivation in an HBsAg-negative patient with clinically resolved hepatitis B virus infection. Liver Int 2010;30:1241–1242.

[27] Hsu C, Tsou HH, Lin SJ, Wang MC, Yao M, Hwang WL, et al. Chemotherapy-induced hepatitis B reactivation in lymphoma patients with resolved HBV infection: a prospective study. Hepatology 2014;59:2092–2100.
[28] Pollicino T, Raffa G, Costantino L, Lisa A, Campello C, Squadrito G, et al. Molecular and functional analysis of occult hepatitis B virus isolates from patients with hepatocellular carcinoma. Hepatology 2007;45:277–285.
[29] Scaglioni PP, Melegari M, Wands JR. Biologic properties of hepatitis B viral genomes with mutations in the precore promoter and precore open reading frame. Virology 1997;233:374–381.
[30] Hadziyannis SJ, Vassilopoulos D. Hepatitis B e antigen-negative chronic hepatitis B. Hepatology 2001;34:617–624.
[31] Milich DR, Chen MK, Hughes JL, Jones JE. The secreted hepatitis B precore antigen can modulate the immune response to the nucleocapsid: a mechanism for persistence. J Immunol 1998;160:2013–2021.
[32] Chu CJ, Lok AS. Clinical significance of hepatitis B virus genotypes. Hepatology 2002;35:1274–1276.

J Gastroenterol (2014) 49:1578–1587
DOI 10.1007/s00535-014-0936-0

The Japanese Society of Gastroenterology

ORIGINAL ARTICLE—LIVER, PANCREAS, AND BILIARY TRACT

Comparison of systems for assessment of post-therapeutic response to sorafenib for hepatocellular carcinoma

Tadaaki Arizumi · Kazuomi Ueshima · Haruhiko Takeda · Yukio Osaki · Masahiro Takita · Tatsuo Inoue · Satoshi Kitai · Norihisa Yada · Satoru Hagiwara · Yasunori Minami · Toshiharu Sakurai · Naoshi Nishida · Masatoshi Kudo

Received: 23 August 2013 / Accepted: 9 January 2014 / Published online: 6 February 2014

Abstract
Background To test the hypothesis that use of the response evaluation criteria in cancer of the liver (RECICL), an improved evaluation system designed to address the limitations of the response evaluation criteria in solid tumors 1.1 (RECIST1.1) and modified RECIST (mRECIST), provides for more accurate evaluation of response of patients with hepatocellular carcinoma (HCC) to treatment with sorafenib, a molecularly targeted agent, as assessed by overall survival (OS).
Methods The therapeutic response of 156 patients with advanced HCC who had been treated with sorafenib therapy for more than 1 month was evaluated using the RECIST1.1, mRECIST, and RECICL. After categorization as showing progressive disease (PD), stable disease (SD), or objective response, the association between OS and categorization was examined using the Kaplan–Meier method to develop survival curves. The 141 cases categorized as PD or SD by the RECIST1.1, but objective response by the mRECIST and RECICL, were further analyzed for determination of the association between OS and categorization.
Results Only categorization using the RECICL was found to be significantly correlated with OS ($p = 0.0033$). Among the patients categorized as SD or PD by the RECIST1.1, reclassification by the RECICL but not the mRECIST was found to be significantly associated with OS and allowed for precise prediction of prognosis ($p = 0.0066$).
Conclusions Only the use of the RECICL allowed for identification of a subgroup of HCC patients treated with sorafenib with improved prognosis. The RECICL should, therefore, be considered a superior system for assessment of therapeutic response.

Keywords Hypervascular lesion · Liver cirrhosis · Response evaluation criteria in solid tumors · Response evaluation criteria in cancer of the liver · Tumor viability

Abbreviations

CE-CT	Contrast-enhanced computed tomography
CI	Confidence interval
CR	Complete response
DCR	Disease control rate
Gd-EOB-DTPA	Gadolinium ethoxybenzyl diethylenetriamine pentaacetic acid
HCC	Hepatocellular carcinoma
mRECIST	Modified RECIST
MRI	Magnetic resonance imaging
OR	Objective response
ORR	Objective response rate
OS	Overall survival
PD	Progressive disease
PR	Partial response

Electronic supplementary material The online version of this article (doi:10.1007/s00535-014-0936-0) contains supplementary material, which is available to authorized users.

T. Arizumi · K. Ueshima · M. Takita · T. Inoue · S. Kitai · N. Yada · S. Hagiwara · Y. Minami · T. Sakurai · N. Nishida · M. Kudo (✉)
Department of Gastroenterology and Hepatology, Kinki University Faculty of Medicine, 377-2 Ohno-higashi, Osaka-sayama, Osaka 589-8511, Japan
e-mail: m-kudo@med.kindai.ac.jp

H. Takeda · Y. Osaki
Department of Gastroenterology and Hepatology, Osaka Red Cross Hospital, 5-53 Fudegasaki-cho, Tennoji-ku, Osaka 543-8555, Japan

SD	Stable disease
RECICL	Response evaluation criteria in cancer of the liver
RECIST1.1	Response evaluation criteria in solid tumors 1.1
RFA	Radiofrequency ablation

Introduction

Hepatocellular carcinoma (HCC) is the third most common cause of cancer mortality worldwide [1], and a considerable number of patients continue to be diagnosed with advanced disease. Recently, sorafenib has been shown to improve the survival of patients with advanced-stage HCC [2]. The effectiveness is attributed to its unique antiproliferative and antiangiogenic mechanism [3–9].

Although the extent of tumor reduction observed with sorafenib therapy has been unsatisfactory, previous trials found that sorafenib significantly improved overall survival (OS) [2, 10]. Indeed, it has become well known that improvement in objective response (OR) without shrinkage of a tumor is a unique characteristic of this drug. As reduction in tumor vascularity appears to be direct effect of sorafenib, it is reasonable to speculate that the longer OS obtained with sorafenib can be attributed to its unique antiangiogenic mechanism, in addition to its antiproliferative effect on cancer cells. As increased tumor viability is typically accompanied by an increase in arterial vascularity, evaluation of arterial enhancement on imaging is critical in predicting OS. However, the response evaluation criteria in solid tumors 1.1 (RECIST1.1), the first set of criteria developed for assessment of response to treatment by HCC patients, focuses on assessment of tumor size and neglects consideration of changes in vascularity status.

In recognition that the vascularity of a lesion is important in evaluating response to HCC treatment, the modified-RECIST (mRECIST) requires assessment of tumor vascularity, which reflects the extent of tumor necrisis [11, 12]. However, use of the mRECIST still poses a difficulty in measuring irregularly shaped tumors, because it calls for unidirectional measurement of tumor size for overall evaluation of tumor burden. Therefore, use of the mRECIST, as well as the RECIST1.1, may not provide for completely adequate evaluation of tumor response in HCC patients.

To overcome the disadvantages of using the conventional criteria, we designed the response evaluation criteria in cancer of the liver (RECICL), a new evaluation system based on evaluation of change in tumor vascularity together with 2-directional assessment of tumor size. Due to the inclusion of these criteria, we hypothesized that use of the RECICL provides for more accurate evaluation of response to sorafenib therapy as assessed by OS than the RECIST1.1 or mRECIST. By testing this hypothesis, we attempted to fulfill 2 research aims in the present study. First, we endeavored to determine the means by which the therapeutic response of HCC patients, especially those presenting with hypervascular lesions and/or with lesions of irregular shape, should be estimated in the context of accurate prediction of OS. Second, we attempted to clarify the significance of and identify any problems with the use of the RECICL by retrospective comparison of its use with that of the RECIST1.1 and mRECIST criteria for evaluation of response among the same cohort of HCC patients.

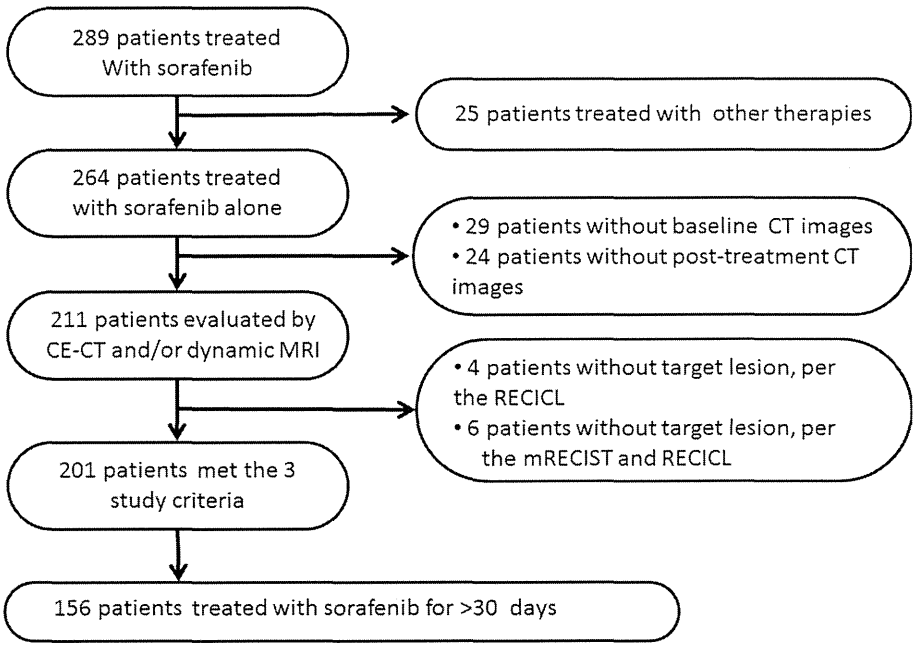

Fig. 1 Flow chart of patient selection process. After exclusion of patients who met the exclusion criteria or did not meet the inclusion criteria, 156 patients remained for analysis

Materials and methods

Patients

Between May 2009 and August 2011, 289 patients with advanced HCC had been treated with sorafenib therapy at Kinki University Hospital or Osaka Red Cross Hospital. From among these patients, 156 patients who had undergone continuous administration of sorafenib for more than 1 month and met the inclusion criteria were selected for study enrollment. The response of all patients to sorafenib had been examined at least once using contrast-enhanced computed tomography (CE-CT) and/or dynamic magnetic resonance imaging (MRI), both are imaging techniques (Fig. 1). Patients' characteristics are summarized in Table 1. Our institution did not require institution approval or informed consent for review of patient records and images in this retrospective study. We posted research content at outpatient areas and a website, and we gave patients the right to refusal for our study.

The inclusion criteria for this study were (1) diagnosis of HCC based on histological examination or radiologic findings showing early enhancement, followed by late wash-out on CE-CT or dynamic MRI, in conjunction with HCC refractory to radiofrequency ablation (RFA) and transarterial chemoembolization based on the indication of sorafenib; (2) performance status of 0 or 1; and (3) Child-Pugh class A or B liver cirrhosis. The exclusion criteria were (1) concomitant antineoplastic treatment; (2) transarterial chemoembolization or RFA performed less than 3 months before initiation of sorafenib; (3) lack of response evaluation using CE-CT or dynamic MRI during follow-up period; or (4) both the presence of extrahepatic lesions and the absence of intrahepatic lesions.

Initial and follow-up assessment

Liver function and tumor stage were evaluated using the Child-Pugh, Barcelona Clinic for Liver Cancer, and Cancer of the Liver Italian Program classifications. Two independent radiologists evaluated tumor size and vascularity every 4–6 weeks during and after treatment using the images of CE-CT and gadolinium ethoxybenzyl diethylenetriamine pentaacetic acid (Gd-EOB-DTPA)-MRI. In this study, we retrospectively determined the best response during the sorafenib treatment and adopted it as the overall response. The responses of all patients were evaluated using RECIST1.1, mRECIST, and RECICL criteria by evaluators who were not blind to the patients' diagnoses. The target lesions of each case were defined by 2 physicians by review of CE-CT and/or dynamic MRI images obtained during pretreatment. OS analysis was based on the length of time from initial treatment until time of death,

Table 1 Characteristics of hepatocellular carcinoma patients treated with sorafenib

	Number of cases (%)
Age	
Median (25–75 %)	73 (66–78)[a]
Gender	
Male	120 (76.9)
Female	36 (23.1)
ECOG PS	
0	150 (96.2)
1	5 (3.2)
2	1 (0.6)
Child-Pugh class	
A	129 (82.7)
B	27 (17.3)
Virus status[b]	
HBV	22 (14.1)
HCV	90 (57.7)
Virus negative	44 (28.2)
TNM stage	
I	5 (3.2)
II	34 (21.8)
IIIA	33 (21.2)
IIIB	4 (2.6)
IIIC	29 (18.6)
IV	51 (32.7)
CLIP score	
0	6 (3.8)
1	59 (37.8)
2	54 (28.9)
3	26 (16.7)
4	10 (6.4)
5	1 (0.6)
BCLC stage	
A	39 (25)
B	36 (23.1)
C	81 (51.9)
Starting dose of sorafenib (mg)	
200	4 (2.6)
400	83 (53.2)
800	69 (44.2)
Total dose of sorafenib (g)	
Median (25–75 %)	66.8 (38.8–135.6)[a]
Serum AFP level (ng/m)	
Median (25–75 %)	115 (12–2230)[a]
Serum DCP (mAU/ml)	
Median (25–75 %)	786 (46–4853)[a]

ECOG Eastern Cooperative Oncology Group, *PS* performance status, *AFP* alpha fetoprotein, *DCP* des-gamma carboxyprothrombin, *BCLC* Barcelona Clinic for Liver Cancer, *CLIP* Cancer of the Liver Italian Program, *HBV* hepatitis B virus, *HCV* hepatitis C virus

[a] Dispersion variables are shown as median values (25–75 %)

[b] Cases testing positive for hepatitis B virus surface antigen (HBsAg) were regarded as cases of HBV-related HCC and cases testing positive for hepatitis C antibody (HCV Ab) were regarded as cases of HCV-related HCC

and OS analysis of patients who were alive at the end of the observation was based on the length of time from initial treatment until time of the final hospital visit.

Response evaluation using the RECIST1.1, mRECIST, and RECICL

The differences among the RECIST1.1, mRECIST, and RECICL are summarized in Supplementary Table 1. Briefly, both the RECIST1.1 and mRECIST call for unidirectional measurement of tumors, but the RECIST1.1 does not require evaluation of tumor viability while the mRECIST requires evaluation of only those areas of the tumor showing arterial enhancement on CE-CT or dynamic MRI. In contrast, the RECICL requires 2-directional measurement of tumors showing arterial enhancement. Representative images of the cases evaluated by the RECIST1.1, mRECIST, and RECICL are shown in Supplementary Figure 1. As can be observed, use of the RECIST1.1 called for unidirectional measurement of both enhanced and necrotic lesions, which showed no change before and after treatment (Supplementary Figures 1A and 1B). On the other hand, use of the mRECIST and RECICL required evaluation of tumor enhancement, which revealed a response according to the mRECIST and RECICL criteria (Supplementary Figures 1C and 1D for mRECIST and Supplementary Figures 1E and 1F for RECICL). Unlike the mRECIST, which does not require evaluation of lesions that do not show enhancement, the RECICL considers tumors not showing enhancement to be viable if they increase in size after initiation of therapy, as demonstrated in Supplementary Figure 2.

Definition of terms

Complete response (CR) was defined as disappearance of all lesions by the RECIST1.1, as disappearance of any arterial enhancement within all target lesions by the mRECIST, and as either a 100 % tumor necrotizing effect or a 100 % reduction in tumor size accompanied by disappearance of all contrast enhancement at any phase by the RECICL. Partial response (PR) was defined as 30 % or greater decrease in tumor size as determined by evaluation of the sum of the diameters of the target lesions, whose size was estimated using unidirectional measurement, by both the RECIST1.1 and mRECIST, and as 50 % or greater reduction in tumor necrosis or size as determined by 2-directional measurement by the RECICL. Progressive disease (PD) was defined as 20 % or greater increase in tumor size as determined by evaluation of the sum of the maximal dimensions of the target lesions by both the RECIST1.1 and mRECIST and as either a 25 % or greater increase in tumor size or the appearance of 1 or more new lesions by the RECICL. The RECIST1.1, mRECIST, and the RECICL all defined stable disease (SD) as the absence of either PR or PD; OR as the sum of all cases showing CR and PR; objective response rate (ORR) as the percentage of OR among all cases; and disease control rate (DCR) as the percentage of cases showing CR, PR, or SD.

Statistical analysis

Univariate survival curves were estimated using the Kaplan–Meier method, comparison of survival rates among groups was conducted using the log-rank test, and comparison of categorical variables was performed using the Chi Square test. The level of significance was set at $p < 0.05$. All analyses were performed using SAS statistical software version 8.2 (SAS Institute, Cary, NC, USA) or the SPSS Medical Pack for Windows version 10.0 (SPSS, Inc., Chicago, IL, USA).

Results

Evaluation of response by the RECIST1.1, mRECIST, and RECICL

Of the 156 patients who had been successfully treated with sorafenib therapy for more than 30 days, the number of patients showing CR, PR, SD, and PD and the ORR and DCR as estimated by use of each system were, respectively, as follows: 3, 12, 71, and 70 cases and 9.6 % and 55.1 % according to the RECIST1.1; 6, 30, 55, and 65 cases and 23.1 % and 58.3 % according to the mRECIST; and 6, 29, 53, and 68 cases and 22.4 % and 56.4 % according to the RECICL (Tables 2, 3). Although no statistically significant difference was observed among the DCR estimated by the 3 systems, 20 patients (approximately 14 %) classified as SD by the RECIST1.1 were classified as OR by the mRECIST and RECICL.

Table 2 Classification of response to sorafenib by the RECIST1.1, mRECIST, and RECICL

	Number of patients				Percentage (%)	
	CR	PR	SD	PD	ORR	DCR
RECIST1.1	3	12	71	70	9.6	55.1
mRECIST	6	30	55	65	23.1	58.3
RECICL	6	29	53	68	22.4	56.4

The number of the patients classified as CR, PR, SD, and PD using each system are shown. Objective response rate (ORR) is the percentage of patients evaluated as CR or PR. Disease control rate (DCR) is the percentage of patients evaluated as CR, PR, or SD

Table 3 Comparisons of the response classification between RECIST1.1 and RECICL (A), and between mRECIST and RECICL (B)

	No. of patients (%)				
	RECICL				Total RECIST1.1 evaluation
	CR	PR	SD	PD	
(A) RECIST1.1					
CR	3 (1.9)				3 (1.9)
PR	2 (1.3)	10 (6.4)			12 (7.7)
SD	1 (0.6)	17 (10.9)	51 (32.7)	2 (1.3)	71 (45.5)
PD		2 (1.3)	2 (1.3)	66 (42.3)	70 (44.9)
Total RECICL evaluation	6 (3.8)	29 (18.6)	53 (34.0)	68 (43.6)	156
	No. of patients (%)				
	RECICL				Total mRECIST evaluation
	CR	PR	SD	PD	
(B) mRECIST					
CR	6 (3.8)				6 (3.8)
PR		28 (17.9)		2 (1.3)	30 (19.2)
SD		1 (0.6)	51 (32.7)	3 (1.9)	55 (35.3)
PD			2 (1.3)	63 (40.4)	65 (41.7)
Total RECICL evaluation	6 (3.8)	29 (18.6)	53 (34.0)	68 (43.6)	156

Comparison of Kaplan–Meier curves for OS as estimated by the RECIST1.1, mRECIST, and RECICL

Figure 2 shows the Kaplan–Meier curves for OS as estimated using the 3 systems (Fig. 2a as estimated by the RECIST1.1, Fig. 2b by the mRECIST, and Fig. 2c by the RECICL). The median OS of the patients classified as OR, SD, and PD, respectively, by the 3 systems was 19.9 months [95 % confidence interval (CI) 12.5–21.3 months], 19.2 months (95 % CI 15.1–23.3 months), and 14.3 months (95 % CI 9.7–18.8 months) by the RECIST1.1; 27.2 months (95 % CI 15.2–39.2), 16.8 months (95 % CI 13.8–19.7 months), and 14.3 months (95 % CI 10.5–18.0) by the mRECIST; and 27.2 months (95 % CI 9.6–44.8 months), 19.2 months (95 % CI 17.1–21.3 months), and 14.3 months (95 % CI 10.1–18.4 months) by the RECICL. As shown in Figs. 2a, b, use of both the RECIST1.1 and mRECIST failed to allow for stratification of OS, although classification of response by the mRECIST was found to be more strongly associated with OS than that by RECIST1.1 ($p = 0.0575$ and $p = 0.073$ by log-rank test, respectively). On the other hand, classification of response by RECICL was found to be significantly associated with OS, with the patients showing OR found to have the longest survival and those showing PD the shortest ($p = 0.0033$ by log-rank test; Fig. 2c; Table 4). Regarding the treatment response determined by RECICL, the OS was significantly higher in the group of OR than in PD patients ($p = 0.002$). However, we could not detect the significant association between SD and OR, and PD for OS, although there were the trends of higher OS in the better response groups (respectively, $p = 0.093$, $p = 0.069$).

Inconsistency among classification by the RECIST1.1, mRECIST, and RECICL

Figure 3 shows the differences in response classification obtained using the RECIST1.1, mRECIST, and RECICL. As can be observed, most patients classified as either PD or SD by RECIST1.1 were classified as either CR or PR (i.e., as OR) by both the mRECIST and RECICL, leading 28 of 156 patients to be classified differently by the RECIST1.1 compared to the mRECIST and RECICL. Specifically, of the 141 patients classified as either PD or SD by the RECIST1.1, 21 of the patients classified as PD and 20 classified as SD were classified as OR by the mRECIST and RECICL (Fig. 3). This finding suggested the possibility that patients classified as OR by the mRECIST and/or RECICL, even those classified as SD or PD by the RECIST1.1, showed better prognosis than those classified as non-OR. To examine this possibility, Kaplan–Meier survival analysis was performed of cases classified as SD or PD by the RECIST1.1 for comparison of their classification by the mRECIST, and RECICL. Among the 141 patients classified as PD or SD by the RECIST1.1, the number of cases of OR, SD, and PD and the ORR and DCR was estimated at 17 cases, 55 cases, and 69 cases and 12.1 %

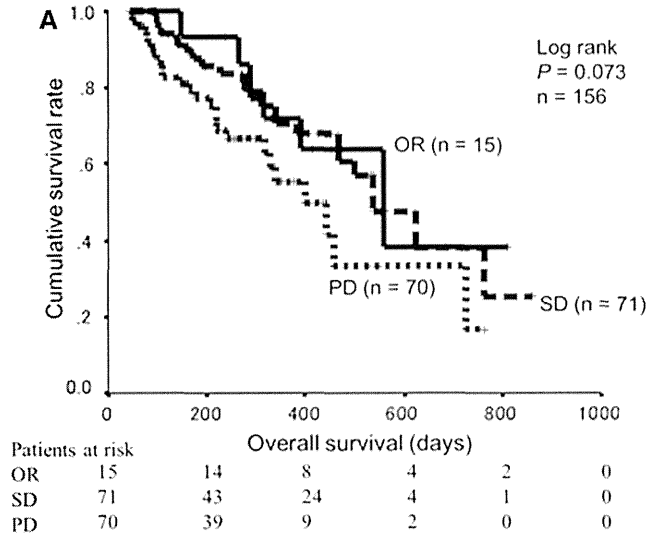

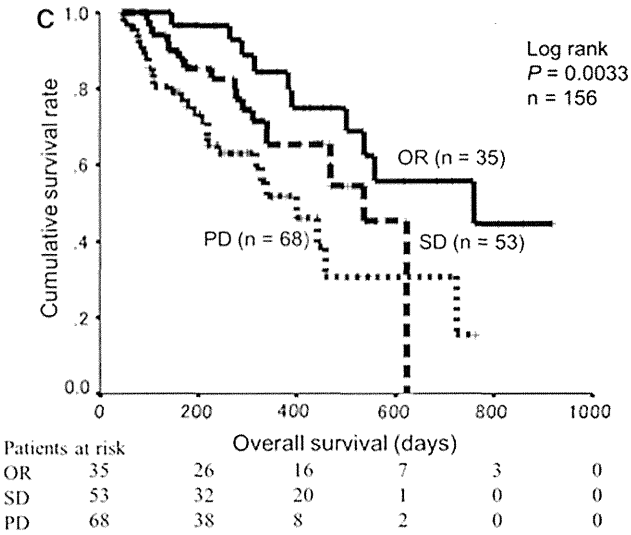

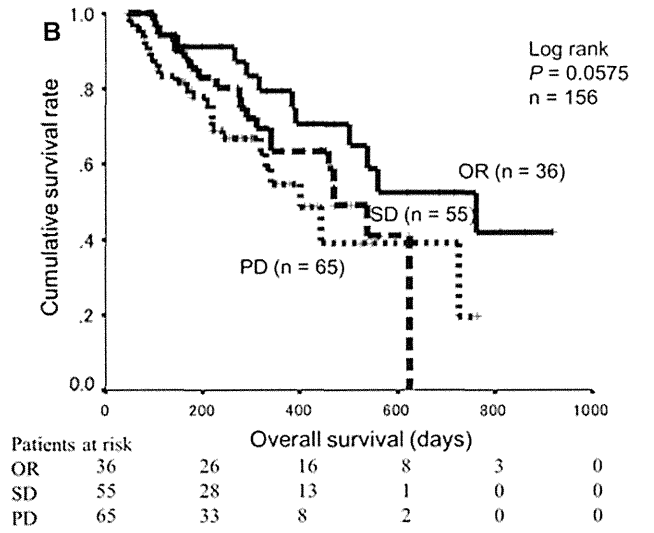

Fig. 2 Kaplan–Meier curves of overall survival based on response to treatment as estimated by the RECIST1.1, mRECIST, and RECICL. Kaplan–Meier curves of the overall survival of the 156 patients based on response to sorafenib therapy as estimated by the RECIST1.1 (**a**), mRECIST (**b**), and RECICL (**c**). The median OS of the patients classified as OR, SD, and PD, respectively, was 19.9 months, 19.2 months, and 14.3 months by the RECIST1.1 ($p = 0.073$ by log-rank test); 27.2 months, 16.8 months, and 14.3 months by the mRECIST ($p = 0.0575$); and 27.2 months, 19.2 months, and 14.3 months by the RECICL ($p = 0.0033$)

and 51.1 %, respectively, by the mRECIST and 15 cases, 56 cses, and 70 cases and 10.1 % and 50.3 %, respectively, by the RECICL.

Figure 4 shows the Kaplan–Meier curve for OS of these 141 patients as estimated by the mRECIST and RECICL. As can be observed, the median OS of patients classified as OR, SD, and PD was 27.2 months (95 % CI 11.7–42.7 months), 16.8 months (95 % CI 13.8–19.7 months), and 14.3 months (95 % CI 10.5–18.0 months), respectively, as estimated by the mRECIST and 27.2 months (95 % CI 11.9–42.5 months), 19.2 months (95 % CI 17.1–21.3 months), and 14.3 months (95 % CI 10.1–18.4 months), respectively, as estimated by the RECICL. Whereas classification of response by the mRECIST failed to allow for stratification of each type of response for OS ($p = 0.1124$; Fig. 4a), classification of response by RECICL was found to be significantly associated with OS, indicating that it allows for precise prediction of prognosis ($p = 0.0066$; Fig. 4b).

Discussion

For management of cancer chemotherapy, it is critical to have reliable tools to guide treatment planning in clinical practice. For this, OS should be considered as a critical

Table 4 Univariate and multivariate analyses for the contribution of clinical backgrounds and tumor response assessed by the three criteria on overall survivals

Variable	$N = 156$	Overall survival (days)		p value	Multivariate analysis		
		Median	95 % CI	Log rank	HR	95 % CI	p value
Age							
<73	77	399	292–505				
≥73	79	533	383–692	0.33			
Gender							
Male	120	409	308–5096				
Female	36	623	240–1005	0.45			
Child-Pugh stage							
A	129	457	359–554				
B	27	340	259–420	0.30			
Virus status†							
HBV	22	468	313–622				
Others	134	399	289–508	0.60			
HCV	90	361	243–478				
Others	66	468	349–586	0.49			
Negative	44	538	298–777				
Others	112	390	271–508	0.74			
TNM stage							
I, II, III	105	468	322–613				
IV	51	361	232–489	0.48			
CLIP score							
0, 1	65	538	–				
2, 3, 4, 5	91	341	238–443	0.004	1.475	0.76–2.86	0.25
0, 1, 2	119	500	418–581				
3, 4, 5	37	274	157–390	<0.001	2.139	1.07–4.24	**0.030**
BCLC stage							
A, B	75	538	338–737				
C	81	390	291–488	0.15			
A	39	–	–				
B, C	117	361	297–424	0.023	1.516	0.73–3.14	0.26
Starting dose of sorafenib (mg)							
200, 400	87	538	286–789				
800	69	409	282–535	0.85			
Total dose of sorafenib (g)							
<70	78	274	150–397				
≥70	78	538	435–640	<0.001	2.829	1.61–4.96	**<0.001**
AFP							
<100	79	500	435–564				
≥100	77	382	317–446	0.19			
DCP							
<800	77	538	453–622				
≥800	79	340	206–473	0.013	1.224	0.71–2.09	0.45
RECIST							
OR	15	–	–				
SD, PD	141	382	294–469	0.032	1.686	0.40–7.00	0.47
OR, SD	86	558	441–674				
PD	70	243	204–281	<0.001	1.284	0.24–6.87	0.77

Table 4 continued

Variable	$N = 156$	Overall survival (days)		p value	Multivariate analysis		
		Median	95 % CI	Log rank	HR	95 % CI	p value
mRECIST							
OR	36	558	337–778				
SD, PD	120	349	285–412	0.015	3.904	0.89–16.959	0.069
OR, SD	91	538	424–651				
PD	65	250	201–298	<0.001	1.274	0.438–3.704	0.65
RECICL							
OR	35	762	–				
SD, PD	121	341	276–405	<0.001	6.398	1.15–35.44	**0.034**
OR, SD	88	558	441–674				
PD	68	241	202–279	<0.001	1.915	0.40–9.10	0.41

The multivariate analysis revealed the CLIP score, a total dose of sorafenib and RECICL, as the independent factor contributing OS

HCV hepatitis C virus, *BCLC* Barcelona Clinic for Liver Cancer, *AST* aspartate aminotransferase, *ALT* alanine aminotransferase, *AFP* alpha fetoprotein, *DCP* des-gamma carboxyprothrombin

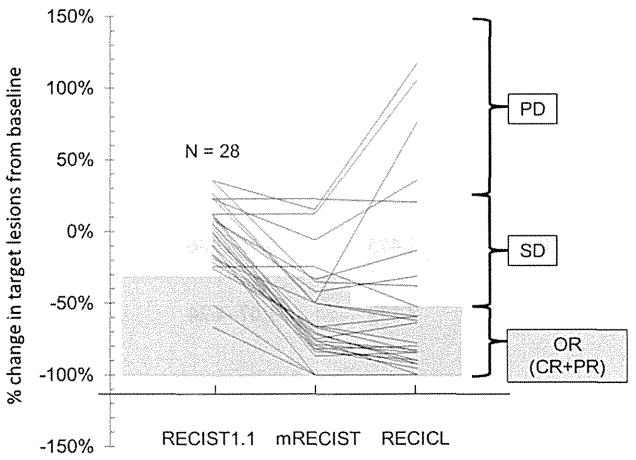

Fig. 3 Percentage change in tumor size of cases classified differently by the RECIST1.1, mRECIST, and RECICL. Percentage change in tumor size of 28 cases that were categorized differently by the RECIST1.1, mRECIST, and RECICL. The percentage change was calculated using the formula (tumor size post treatment – tumor size pretreatment)/tumor size pretreatment × 100 for estimation by the RECIST1.1 and mRECIST and the formula (tumor area post treatment—tumor area pretreatment/tumor area pretreatment × 100 for estimation by the RECICL. The *lower part* of the panel denotes the range of objective response (OR), the middle part of the panel the range of stable disease (SD), and the *upper part* the range of progressive disease (PD)

endpoint, although tumor response assessed by imaging was sometimes used as a surrogate endpoint so far. When the validity of the criteria in predicting OS in advanced HCC patients treated with sorafenib was compared, we found RECICL was the best criteria for the precise prediction of the prognosis of these patients compared to the RECIST1.1 and mRECIST.

In Western countries, World Health Organization criteria and the RECIST1.1 are commonly used for evaluation of treatment for liver cancer [13]. While their use has proven valuable in assessing response to conventional cytotoxic chemotherapy, there has been concern regarding their applicability to patients treated with recently developed molecularly targeted agents, such as sorafenib, which appear to have a "dormant" effect in that they initially appear to yield little response but ultimately lead to improvement in overall time to progression and OS [2, 10]. Sorafenib in particular has been a breakthrough agent in the treatment of advanced HCC, as demonstrated by the significant improvement in OS, despite the reporting of an ORR of only 2 % with its use [2, 10]. This observation of increased response to treatment has prompted use of imaging techniques, namely CE-CT and MRI, as an alternative method of assessing treatment response [14, 15]. While both mRECIST and RECICL incorporate vascularity as a factor in response assessment, the RECICL also calls for 2-directional measurement of tumor size and defines tumors that increase in size to be viable even if they do not show early enhancement upon imaging. The major advantage of use of the mRECIST and RECICL is that these call for evaluation of the contrast-enhancing portion of the tumor rather than evaluation of the entire tumor (Supplementary Figure 1) and consider tumor necrosis a sign of response. Such differences in criteria results in the ORR estimated using the mRECIST or RECICL to be approximately 2.5 times higher than that estimated using the RESICT1.1. Interestingly, the most significant association between tumor response and OS was found using the RECICL (Fig. 2c), although classification by mRECIST was found to be more strongly associated with

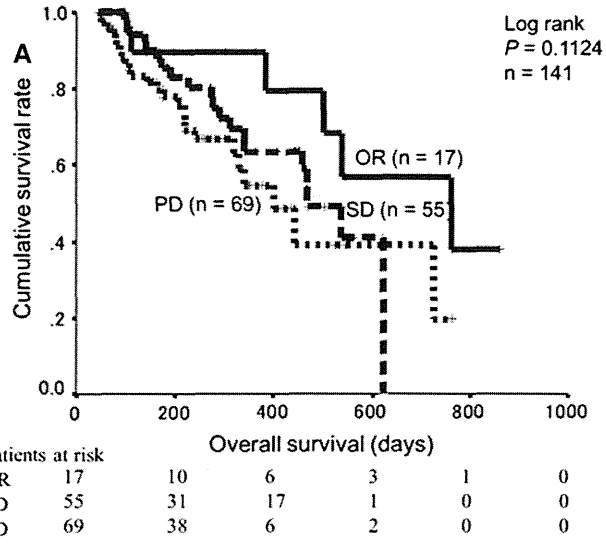

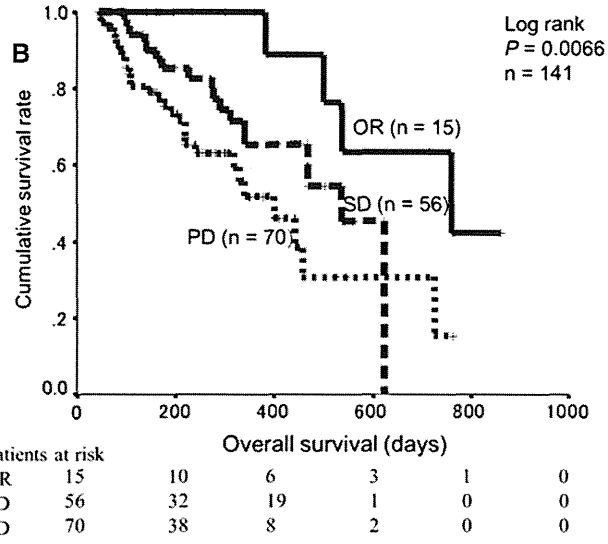

Fig. 4 Kaplan-Meier curves of overall survival of patients classified as SD or PD by the RECIST1.1 and as OR by the mRECIST and RECICL. Kaplan-Meier curves of 141 patients classified as SD or PD by the RECIST1.1 and as OR by the mRECIST (**a**) and RECICL. The median OS of patients classified as OR, SD, and PD was 27.2 months, 16.8 months, and 14.3 months, respectively, as estimated by the mRECIST ($p = 0.1124$ by log-rank test) and 27.2 months, 19.2 months, and 14.3 months, respectively, as estimated by the RECICL ($p = 0.0066$)

classification by RESICT1.1 (Fig. 2a, b). Therefore, it is reasonable to speculate that evaluation of tumor viability improves assessment of the antitumor activity of sorafenib by the mRECIST and RECICL but not by the RECIST1.1.

Another difference between the mRECIST and RECICL is that, while classification of response by the former is based on unidirectional measurement, that by the latter is based on 2-directional measurement. Moreover, while only the hypervascular area of the tumor is regarded as viable, and, thus, tumor viability is only estimated during the arterial phase, by the mRECIST, tumor viability is estimated at all phases by the RECICL. Supplementary Figs. 2 and 3 show examples of how use of the mRECIST and RECICL can lead to different classification of the same cases. In the case shown in Supplementary Fig. 3, marked reduction of tumor volume with enhancement was observed. Although the response was classified as SD by the mRECIST, it was classified as PR by the RECICL, as assessed by 2-directional measurement of size. Another advantage of using RECICL is that it calls for evaluation of non-enhanced areas of the target lesion, which are often found to have increased on post-therapeutic imaging. Indeed, some lesions that appear hypovascular on CE-CT are found to have increased in size and should, thus, be regarded as viable (Supplementary Figure 2). Therefore, patients classified as PR by the mRECIST would be classified as PD by the RECICL, indicating that use of the RECICL allows for more accurate categorization of response than the mRECIST for assessment of OS. Indeed, use of the RECICL was found to allow for successful discrimination of patients with tumor progression among the patients who had been classified as SD by the mRECIST.

There should be three limitations regarding the assessment by RECICL. First, the assessment of RECICL focus only on the measurable intrahepatic lesions without evaluating the portal vein thrombi and extrahepatic lesions. Second, a hypovascular HCC such as sarcomatoid HCC should be difficult for assessment by RECICL because the alteration of vascularity could not be determined. Evaluation of response for such lesions should be determined using another criteria. Third, the retrospective nature of the study might have led to bias in selection of the patients. To address the limitations and independently validate the results of this study, we are currently designing an investigation of the accuracy of use of the RECICL in the prediction of OS in a prospective multicenter patient cohort with a larger sample size.

In this comparison of the validity of use of the RECIST1.1, mRECIST, and RECICL, use of the RECICL was found to allow for much more precise identification of patients with better prognosis compared to the RECIST1.1 or mRECIST. This finding leads us to conclude that use of the RECICL is the best means of obtaining precise prognostic information at an early stage after treatment. Although further studies are required to confirm the superiority of RECICL in HCC with portal vein thrombi and extrahepatic lesions, the results of this study are of significance from a clinical viewpoint, especially in the selection of therapy. Given the robustness of the data

presented herein, we strongly assert that the RECICL should become the standard system used in the evaluation of response to chemotherapy, including molecularly targeted therapies, by HCC patients.

Acknowledgments This work was supported by a Health Labor Sciences Research Grant from the Ministry of Health Labour and Welfare of Japan (H22-Clinical Oncology-General-015).

Conflict of interest The authors declare that they have no conflict of interest.

References

1. El-Serag HB, Rudolph KL. Hepatocellular carcinoma: epidemiology and molecular carcinogenesis. Gastroenterology. 2007;132:2557–76.
2. Llovet JM, Ricci S, Mazzaferro V, et al. SHARP Investigators Study Group. Sorafenib in advanced hepatocellular carcinoma. N Engl J Med. 2008;359:378–90.
3. Sakurai T, Kudo M. Signaling pathways governing tumor angiogenesis. Oncology. 2011;81:24–9.
4. Wilhelm SM, Adnane L, Newell P, et al. Preclinical overview of sorafenib, a multikinase inhibitor that targets both RAF and VEGF and PDGF receptor tyrosine kinase signaling. Mol Cancer Ther. 2008;7:3129–40.
5. Rini BI. Sorafenib. Expert Opin Pharmacother. 2006;7:453–61.
6. Wu H, Huang C, Chang D. Anti-angiogenic therapeutic drugs for treatment of human cancer. J Cancer Mol. 2008;4:37–45.
7. Kano MR, Komuta Y, Iwata C, et al. Comparison of the effects of the kinase inhibitors imatinib, sorafenib, and transforming growth factor-beta receptor inhibitor on extravasation of nanoparticles from neovasculature. Cancer Sci. 2009;100:173–80.
8. Tanaka S, Arii S. Molecularly targeted therapy for hepatocellular carcinoma. Cancer Sci. 2009;100:1–8.
9. Llovet JM, Bruix J. Molecular targeted therapies in hepatocellular carcinoma. Hepatology. 2008;48:1312–27.
10. Cheng AL, Kang YK, Chen Z, et al. Efficacy and safety of sorafenib in patients in the Asia-Pacific region with advanced hepatocellular carcinoma: a phase III randomised, double-blind, placebo-controlled trial. Lancet Oncol. 2009;10:25–34.
11. Lencioni R, Llovet JM. Modified RECIST (mRECIST) assessment for hepatocellular carcinoma. Semin Liver Dis. 2010;30:52–60.
12. Llovet JM, Di Bisceglie AM, Bruix J, et al. Design and endpoints of clinical trials in hepatocellular carcinoma. J Natl Cancer Inst. 2008;100:698–711.
13. The Liver Cancer Study Group of Japan. General rules for the clinical and pathological study of primary liver cancer. 5th ed. Tokyo: Kanehara; 2009 (revised version).
14. Miller AB, Hogestraeten B, Staquet M, et al. Reporting results of cancer treatment. Cancer. 1981;47:207–14.
15. Ebied OM, Federle MP, Carr BI, et al. Evaluation of responses to chemoembolization in patients with unresectable hepatocellular carcinoma. Cancer. 2003;97:1042–50.

PLOS ONE

Deletion of Nardilysin Prevents the Development of Steatohepatitis and Liver Fibrotic Changes

Shoko Ishizu-Higashi[1], Hiroshi Seno[1]*, Eiichiro Nishi[2]*, Yoshihide Matsumoto[1], Kozo Ikuta[1], Motoyuki Tsuda[1], Yoshito Kimura[1], Yutaka Takada[1], Yuto Kimura[1], Yuki Nakanishi[1], Keitaro Kanda[1], Hideyuki Komekado[1], Tsutomu Chiba[1]

1 Department of Gastroenterology and Hepatology, Kyoto University Graduate School of Medicine, Kyoto, Japan, **2** Department of Cardiovascular Medicine, Kyoto University Graduate School of Medicine, Kyoto, Japan

Abstract

Nonalcoholic steatohepatitis (NASH) is an inflammatory form of nonalcoholic fatty liver disease that progresses to liver cirrhosis. It is still unknown how only limited patients with fatty liver develop NASH. Tumor necrosis factor (TNF)-α is one of the key molecules in initiating the vicious circle of inflammations. Nardilysin (N-arginine dibasic convertase; Nrd1), a zinc metalloendopeptidase of the M16 family, enhances ectodomain shedding of TNF-α, resulting in the activation of inflammatory responses. In this study, we aimed to examine the role of Nrd1 in the development of NASH. $Nrd1^{+/+}$ and $Nrd1^{-/-}$ mice were fed a control choline-supplemented amino acid-defined (CSAA) diet or a choline-deficient amino acid-defined (CDAA) diet. Fatty deposits were accumulated in the livers of both $Nrd1^{+/+}$ and $Nrd1^{-/-}$ mice by the administration of the CSAA or CDAA diets, although the amount of liver triglyceride in $Nrd1^{-/-}$ mice was lower than that in $Nrd1^{+/+}$ mice. Serum alanine aminotransferase levels were increased in $Nrd1^{+/+}$ mice but not in $Nrd1^{-/-}$ mice fed the CDAA diet. mRNA expression of inflammatory cytokines were decreased in $Nrd1^{-/-}$ mice than in $Nrd1^{+/+}$ mice fed the CDAA diet. While TNF-α protein was detected in both $Nrd1^{+/+}$ and $Nrd1^{-/-}$ mouse livers fed the CDAA diet, secretion of TNF-α in $Nrd1^{-/-}$ mice was significantly less than that in $Nrd1^{+/+}$ mice, indicating the decreased TNF-α shedding in $Nrd1^{-/-}$ mouse liver. Notably, fibrotic changes of the liver, accompanied by the increase of fibrogenic markers, were observed in $Nrd1^{+/+}$ mice but not in $Nrd1^{-/-}$ mice fed the CDAA diet. Similar to the CDAA diet, fibrotic changes were not observed in $Nrd1^{-/-}$ mice fed a high-fat diet. Thus, deletion of nardilysin prevents the development of diet-induced steatohepatitis and liver fibrogenesis. Nardilysin could be an attractive target for anti-inflammatory therapy against NASH.

Citation: Ishizu-Higashi S, Seno H, Nishi E, Matsumoto Y, Ikuta K, et al. (2014) Deletion of Nardilysin Prevents the Development of Steatohepatitis and Liver Fibrotic Changes. PLoS ONE 9(5): e98017. doi:10.1371/journal.pone.0098017

Editor: Silvia C. Sookoian, Institute of Medical Research A Lanari-IDIM, University of Buenos Aires-National Council of Scientific and Technological Research (CONICET), Argentina

Received November 27, 2013; **Accepted** April 28, 2014; **Published** May 21, 2014

Funding: This work was supported by the Japan Society for the Promotion of Science (JSPS) KAKENHI 21229009, 23300117, 23590937, 24229005, 24590914, 24590916, 24659363, 25112707, 25130706, 25461021, 25860533, and 26293173; Research program of the Project for Development of Innovative Research on Cancer Therapeutics (P-Direct) from the Ministry of Education, Culture, Sports, Science and Technology of Japan; Health and Labour Sciences Research Grants for Research on Intractable Diseases, Hepatitis, and The innovative development and the practical application of new drugs for hepatitis B from the Ministry of Health, Labour and Welfare, Japan; the Funding Program for Next-Generation World-leading Researchers (LS075), Grants-in Aid from the Ministry of Education, Culture, Science, Sports and Technology of Japan; Kobayashi Foundation for Cancer Research; The Naito Foundation; and Princess Takamatsu Cancer Research Foundation (13-24514). The funders had no role in study design, data collection and analysis, decision to publish, or preparation of the manuscript.

Competing Interests: The authors have declared that no competing interests exist.

* E-mail: seno@kuhp.kyoto-u.ac.jp (HS); nishi@kuhp.kyoto-u.ac.jp (EN)

Introduction

Nonalcoholic fatty liver disease (NAFLD) is a condition in which excess fat accumulates in the hepatocytes of patients without a history of alcohol abuse [1]. NAFLD is a hepatic manifestation of metabolic syndromes, such as obesity, type-II diabetes mellitus, and hyperlipidemia. Its prevalence is increasing particularly in the developed countries [1,2]. Nonalcoholic steatohepatitis (NASH) is a severe form of NAFLD, in which liver inflammation is observed and which progresses to liver fibrosis. A part of NAFLD patients develops NASH that leads to liver fibrosis. However, the exact causes and mechanisms of the development of NASH remain unknown.

Recent investigations have suggested a "multi-hit process" model for the development of NASH [3]. Liver inflammation including NASH can be initiated or enhanced by multiple cytokines secreted mainly by Kupffer cells or macrophages [4]. During liver fibrogenesis, myofibroblasts, that are not present in normal liver, also contribute to liver fibrogenesis through the remodeling of extracellular matrix [5]. In pro-inflammatory cascades, there are several key factors that play a crucial role in initiating or halting inflammation. Tumor necrosis factor (TNF)-α is one of such key molecules, and anti-TNF-α therapies are used widely to treat human inflammatory disorders, such as rheumatoid arthritis and inflammatory bowel diseases [6,7]. To activate TNF-α, a membrane-bound pro-TNF-α must be appropriately and sufficiently cleaved by the prototypical sheddase, TNF-α-converting enzyme (TACE) [8]. Previously, we showed that nardilysin (N-arginine dibasic convertase; Nrd1), a zinc metalloendopeptidase of the M16 family that ubiquitously localizes in various organs, enhances the shedding of TNF-α through TACE activation [9–13]. Nardilysin binds to TACE and directly enhances its catalytic activity [10,11]. It also promotes the ectodomain shedding of

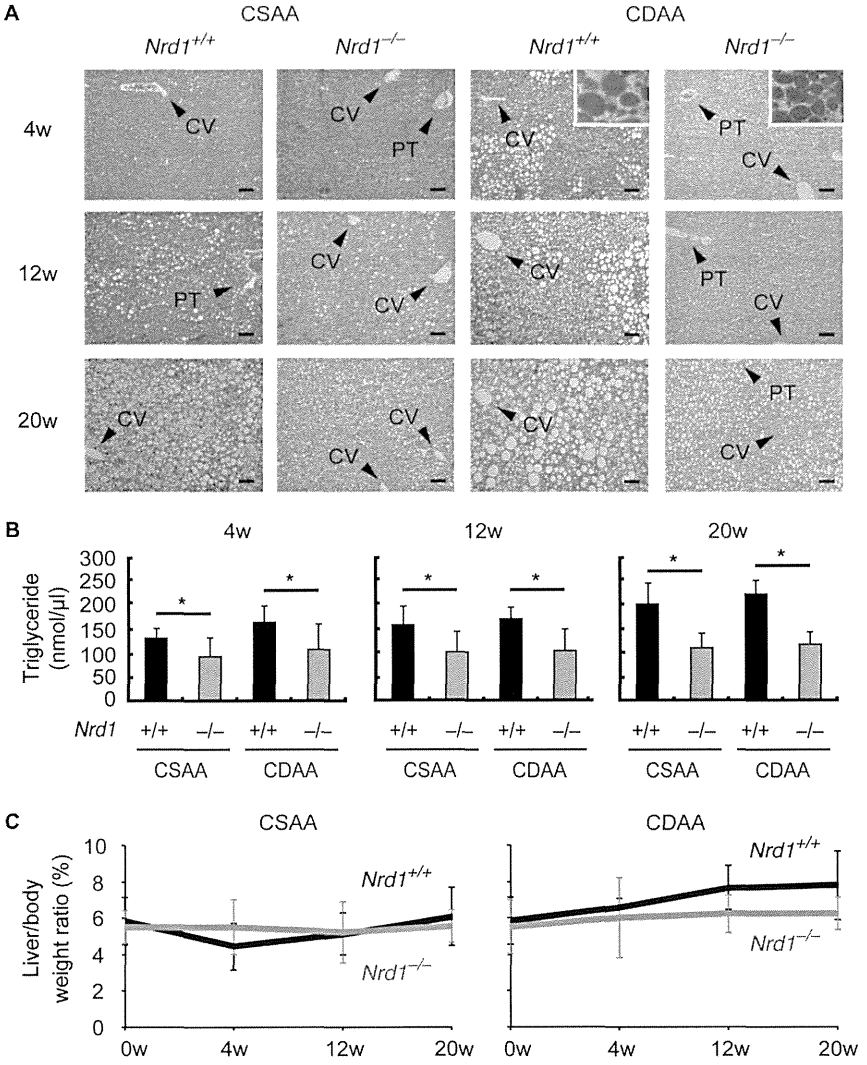

Figure 1. CDAA diet caused hepatic steatosis in *Nrd1*$^{+/+}$ and *Nrd1*$^{-/-}$ mice. A. Histology of the livers of *Nrd1*$^{+/+}$ and *Nrd1*$^{-/-}$ mice fed the CSAA (left) or CDAA (right) diets. Representative changes of the liver with regard to fat deposition at 4 (upper), 12 (middle), and 20 (lower) weeks during the experiments are depicted. Fat deposits were confirmed by oil red O staining shows (orange, inset). CV indicates central vein, and PT marks portal triad. Bars indicate 100 μm. B. Quantification of triglyceride in the liver. Triglyceride in the liver was increased in the livers of both *Nrd1*$^{+/+}$ and *Nrd1*$^{-/-}$ mice during administration of the CDAA or CSAA diets, although it was significantly more prominent in *Nrd1*$^{+/+}$ mice. n = 4–5, each. *$P<0.05$. C. There was no significant difference in the liver/body weight ratio between *Nrd1*$^{+/+}$ and *Nrd1*$^{-/-}$ mice during the experiments.
doi:10.1371/journal.pone.0098017.g001

TNF-α, resulting in activation of the TNF-α/nuclear factor-κB pro-inflammatory signaling cascade [12].

In this study, we aimed to elucidate the mechanisms that distinguish NASH from simple liver steatosis. We examined the role of nardilysin, that is known to enhance TNF-α shedding, in the development of steatohepatitis using *Nrd1*$^{+/+}$ and *Nrd1*$^{-/-}$ mice fed a choline-deficient and amino acid-defined (CDAA) diet and a high-fat diet (HFD), that are used widely to reproduce the natural course of NASH and liver fibrosis in mice as well as in humans.

Materials and Methods

Ethics statement

All animal experiments were undertaken in accordance with institutional guidelines. The Review Board of Kyoto University granted ethical approval for this study.

Animal models

Nardilysin-deficient (*Nrd1*$^{-/-}$) mice (CDB0466K: http://www.cdb.riken.jp/arg/mutant%20mice%20list.html) were previously described [13]. Male *Nrd1*$^{+/+}$ and *Nrd1*$^{-/-}$ mice with the BL6/CBA background were bred and housed in a temperature- and light-controlled facility with unlimited access to food and water. To induce steatohepatitis and liver fibrotic changes, 10–12-week old male mice were fed a control choline-supplemented amino acid-defined (CSAA) diet or a choline-deficient amino acid-defined (CDAA) diet (Research Diets, New Brunswick, NJ, USA) for 4, 12, or 20 weeks according to the previous reports [14,15]. As another diet-induced model of steatohepatitis and liver fibrosis, mice were fed a HFD (Oriental Bio Service, Kyoto, Japan) for 20 weeks on the basis of previous studies [16,17]. Triglyceride levels in the livers were determined with Triglyceride Quantification kit (Abcam, Cambridge, MA, USA) according to the manufacture's protocol. Serum levels of alanine aminotransferase (ALT) were

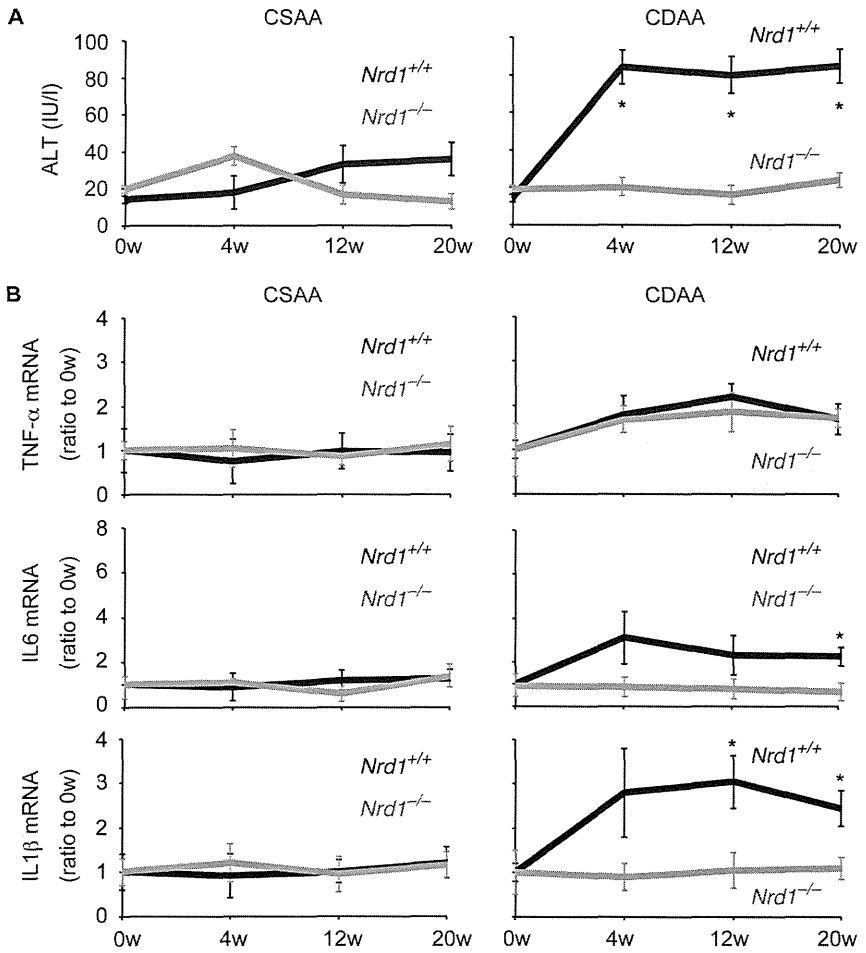

Figure 2. CDAA diet did not cause steatohepatitis in *Nrd1*$^{-/-}$ mice. A. Serum ALT was not elevated in both *Nrd1*$^{+/+}$ and *Nrd1*$^{-/-}$ mice fed the CSAA diet (left). Serum ALT levels were significantly elevated in *Nrd1*$^{+/+}$ mice, but were not elevated in *Nrd1*$^{-/-}$ mice upon administration of the CDAA diet (right). Each value depicts the mean ± standard errors (n = 5–15, each). *$P<0.05$. B. Relative expression of mRNA are shown as relative values compared to those at 0 w. mRNA of TNF-α was increased in both *Nrd1*$^{+/+}$ (significantly) and *Nrd1*$^{-/-}$ mice fed the CDAA diet compared with those fed the CSAA diet, with no significant difference between the two groups. In contrast, the mRNA expression levels of IL6 and IL1-β were increased only in *Nrd1*$^{+/+}$ mice, and these levels were significantly higher than respective values in *Nrd1*$^{-/-}$ mice fed the CDAA diet. (n = 5–16, each) *$P<0.05$.

doi:10.1371/journal.pone.0098017.g002

measured using a Transaminase CII-Test Wako kit (Wako Pure Chemical Industries, Osaka, Japan).

Histological analyses and immunostainings

The liver was resected at various time points, fixed with 4% buffered paraformaldehyde solution, embedded in paraffin, and sectioned into 5-μm thickness. Oil red O (Wako Pure Chemical Industries) staining was performed to confirm fatty deposition. Sirius red (saturated picric acid containing 0.1% Direct Red 80 and 0.1% Fast Green FCF; Sigma-Aldrich, St. Louis, MO, USA) staining was done to visualize collagen deposition. Stained fibrotic areas were measured as percentage area in a representative ×100 high-power field in each mouse using Image J software. For the immunostainings the sections were incubated overnight with the primary antibodies at 4°C, after which the secondary antibodies were added. Kupffer cells or macrophages were stained with rat anti-F4/80 monoclonal antibody (Abcam). TNF-α staining was performed with anti-TNF-α goat polyclonal antibodies (R&D systems, Minneapolis, MN, USA). Activated myofibroblasts were stained with anti-α-smooth muscle actin (SMA) rabbit polyclonal antibody (Abcam). Negative controls were prepared with isotype IgG.

Real-time quantitative reverse transcription-polymerase chain reaction (qRT-PCR)

Total RNA was extracted using Trizol (Life Technologies, Carlsbad, CA, USA). Single-strand complementary DNA (cDNA) was synthesized using a Transcriptor First Strand cDNA Synthesis kit (Roche Applied Science, Basel, Switzerland). qRT-PCR was performed using SYBR Green I Master (Roche Applied Science) and Light Cycler 480 (Roche Applied Science). Values are expressed as arbitrary units relative to glyceraldehyde 3-phosphate dehydrogenase (GAPDH). The primer sets used were: TNF-α-Forward, CCCTCACACTCAGATCATCTTCT, TNF-α-Reverse, GCTACGACGTGGGCTACAG; interleukin (IL) 6-Forward, TAGTCCTTCCTACCCCAATTTCC, IL6-Reverse, TTGGTCCTTAGCCACTCCTTC; IL1-β-Forward, GCAACTGTTCCTGAACTCAACT, IL1-β-Reverse, ATCTTTTGGGGTCCGTCAACT; CCR2-Forward, ATCCACGGCATACTATCAACATC, CCR2-Reverse, CAAGGCTCACCATCATCGTAG; collagen I-For-

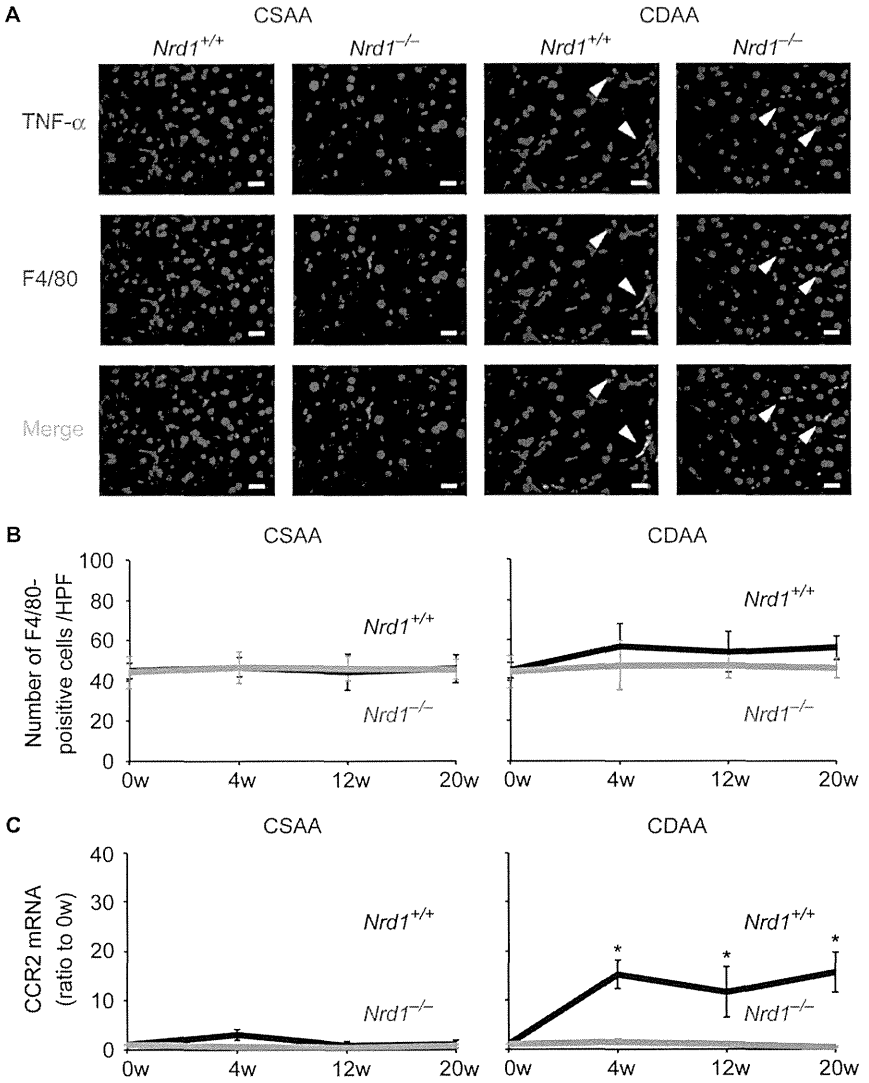

Figure 3. TNF-α was expressed in *Nrd1*$^{+/+}$ and *Nrd1*$^{-/-}$ mice fed the CDAA diet. A. Immunohistochemistry showed that TNF-α protein (red, arrowheads) was expressed in F4/80-positive Kupffer cells or macrophages (green, arrowheads) in the livers of both *Nrd1*$^{+/+}$ and *Nrd1*$^{-/-}$ mouse fed the CDAA diet for 20 weeks (right), but not in mice fed the CSAA diet for 20 weeks (left). A blue color indicates DAPI-positive nuclei. Bars indicate 50 μm. B. The number of F4/80-positive cells/×100 high-power field (HPF) in livers slightly increased (approximately 1.2 times) only in *Nrd1*$^{+/+}$ mice fed the CDAA diet (right). C. Relative expression of mRNA are shown as relative values compared to those at 0 w. The mRNA expression level of CCR2 was increased in *Nrd1*$^{+/+}$ mice fed the CDAA diet, and the levels were significantly higher than respective values in *Nrd1*$^{-/-}$ mice fed the CDAA diet. *$P<0.05$.

doi:10.1371/journal.pone.0098017.g003

ward, GCTCCTCTTAGGGGCCACT, collagen I-Reverse, ATTGGGGACCCTTAGGCCAT; collagen IV-Forward, TCCGGGAGAGATTGGTTTCC, collagen IV-Reverse, CTGGCCTATAAGCCCTGGT; tissue inhibitor of metalloproteinase (Timp) 1-Forward, CTTGGTTCCCTGGCGTACTC, Timp1-Reverse, ACCTGATCCGTCCACAAACAG; transforming growth factor (TGF)-β1-Forward, CTCCCGTGGCTTCTAGTGC, TGF-β1-Reverse, GCCTTAGTTTGGACAGGATCTG; α-SMA-Forward, GTCCCAGACATCAGGGAGTAA, α-SMA-Reverse; TCGGATACTTCAGCGTCAGGA.

Measurement of cytokine levels by enzyme-linked immunosorbent assay (ELISA)

To determine the production and secretion of TNF-α protein in CDAA-treated mouse liver, a modified protocol that described in previous reports was used [18,19]. In brief, a liver fragment was divided into two specimens (100 μg each). One specimen was subjected directly to protein extraction, and the amount of protein extracted was determined using a Bio-Rad protein assay kit (Bio-Rad Laboratories, Hercules, CA, USA). The other was cultured in a 24-well flat-bottomed culture plate in serum-free Dulbecco's modified Eagle's medium (D-MEM; Life Technologies) supplemented with penicillin and streptomycin (Life Technologies). After 12 hours, the supernatant was collected and the protein level measured. The amounts of TNF-α, IL6, and IL1-β proteins were measured using a Mouse ELISA Ready-SET-Go! kit (eBioscience, San Diego, CA, USA) according to the manufacturer's protocol.

Mouse peritoneal macrophage experiments

Mouse peritoneal macrophages were isolated from 8-week-old female C57BL/6J mice. Peritoneal cells were harvested by peritoneal lavage with 10 ml PBS. Cells were re-suspended and

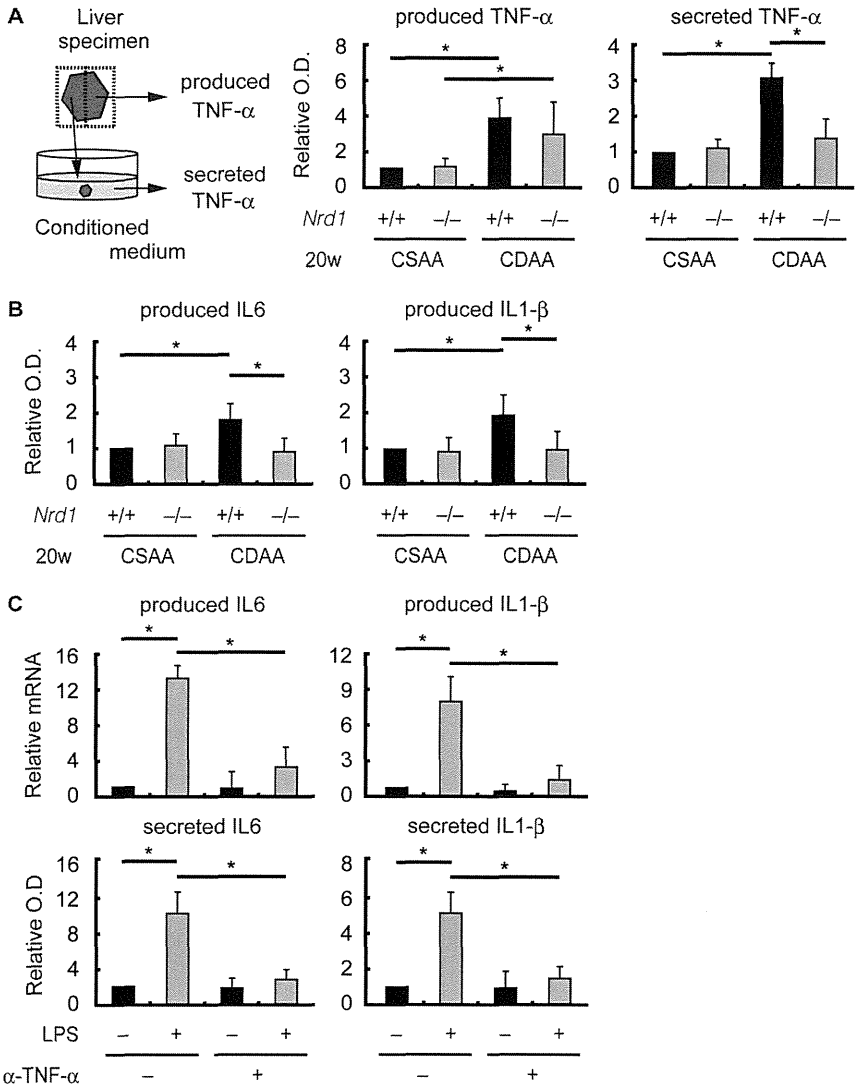

Figure 4. TNF-α was not sufficiently secreted from in *Nrd1*$^{-/-}$ mice fed the CDAA diet. A. A liver fragment was divided into two pieces. One was directly subjected to protein extraction directly and measurement of TNF-α (produced TNF-α). The other piece was cultured in serum-free medium for 12 hours, and the supernatant was subjected to measurement of TNF-α (secreted TNF-α). The relative optical density (O.D.) to that of *Nrd1*$^{+/+}$ fed the CSAA diet was determined by ELISA for TNF-α. Production of TNF-α from liver specimens were not significantly different between *Nrd1*$^{+/+}$ and *Nrd1*$^{-/-}$ mice fed the CDAA diet for 20 weeks ("produced TNF-α"). In contrast, TNF-α secreted from liver specimens was significantly increased in *Nrd1*$^{+/+}$ mice fed the CDAA diet for 20 weeks compared with those fed the CSAA diet; however, the elevation was not observed in *Nrd1*$^{-/-}$ mice under the same condition ("secreted TNF-α"). *$P<0.05$. B. Production of IL6 and IL1-β proteins were significantly increased only in *Nrd1*$^{+/+}$ mice fed the CDAA diet for 20 weeks compared with those in *Nrd1*$^{-/-}$ mice fed the CSAA diet for 20 weeks. *$P<0.05$. C. mRNA (upper, 'produced') and protein (lower, 'secreted') production of IL6 and IL1-β were significantly increased after LPS treatment in *Nrd1*$^{+/+}$ mouse peritoneal macrophages. However, administration of anti-TNF-α neutralizing antibodies significantly suppressed the production of IL6 and IL1-β in the presence of LPS. *$P<0.05$.
doi:10.1371/journal.pone.0098017.g004

cultured in D-MEM supplemented with 10% FCS, 100 mg/ml of penicillin, 100 mg/ml of streptomycin, and 1.25 μg/ml of amphotericin B. 1.0×10^6 peritoneal cells were seeded into a 48-well dish, and incubated for 2 hours. Then, cells were washed in PBS, and re-cultured in the serum-free medium. To inhibit TNF-α activity, either control serum or 0.4 μg/ml of anti-TNF-α neutralizing polyclonal antibodies (R&D systems) was administered into the culture medium. After 30 minutes later, 1 μg/ml of lipopolysaccharide (LPS) were added. Medium and cells were collected 2 hours after the stimulation, and subjected to the analyses according to the methods described above.

Statistical analyses

Results are the mean ± standard deviation unless stated otherwise. Differences between treatments, groups, and strains were analyzed using the two-tailed Student's t-test.

Results

Nrd1$^{-/-}$ mice did not develop steatohepatitis with CDAA diet

The CDAA diet is deficient in choline only, but contains methionine, allowing observation of the sequential development of steatohepatitis and liver fibrotic changes in a longer experimental

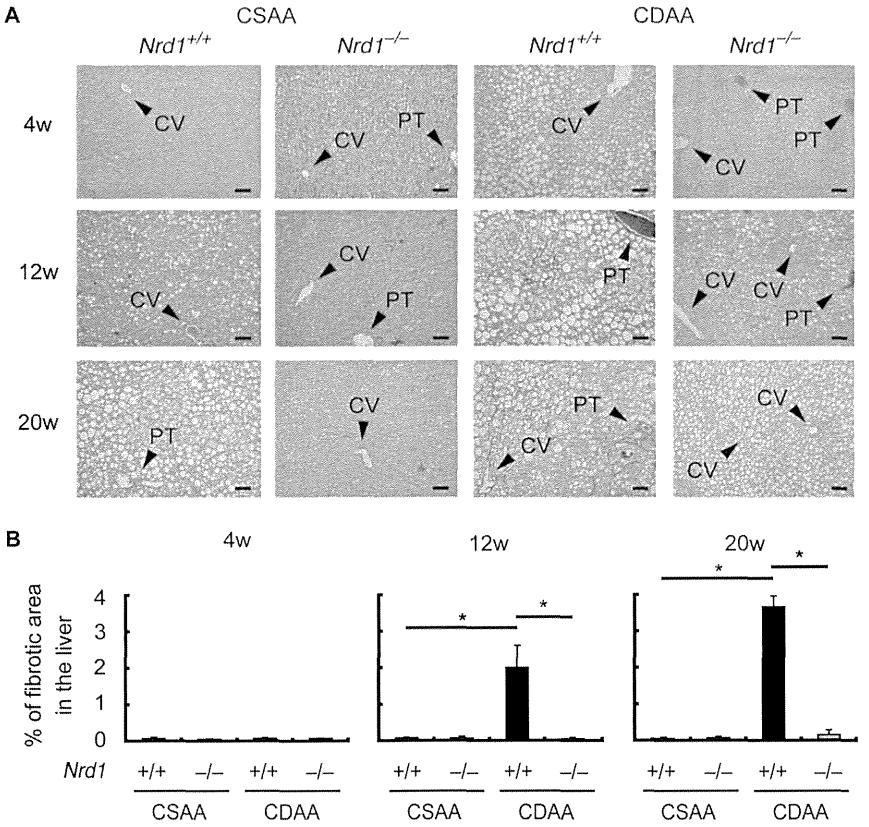

Figure 5. Liver fibrotic area was not observed in *Nrd1*$^{-/-}$ mice fed the CDAA diet. A. Liver fibrosis was determined by Sirius red staining (red) in *Nrd1*$^{+/+}$ and *Nrd1*$^{-/-}$ mice at 4 (upper), 12 (middle), and 20 (lower) weeks in the livers of *Nrd1*$^{+/+}$ and *Nrd1*$^{-/-}$ mice fed the CSAA or CDAA diet. Fibrotic changes were not observed in *Nrd1*$^{+/+}$ or *Nrd1*$^{-/-}$ mice fed the CSAA diet (left). Fibrotic changes were prominent in *Nrd1*$^{+/+}$ mice, but not in *Nrd1*$^{-/-}$ mice fed the CDAA diet (right). Bars indicate 100 μm. B. Quantification of fibrotic areas. Fibrotic areas was observed and increased in a time-dependent manner only in the livers of *Nrd1*$^{+/+}$ mice fed the CDAA diet. n = 5–8, each. *P<0.05.
doi:10.1371/journal.pone.0098017.g005

period in mice [4,14]. The control CSAA diet also causes mild steatosis, but does not result in steatohepatitis and liver fibrotic changes in mice [4,14]. To study the role of nardilysin during the development of steatohepatitis followed by liver fibrosis, *Nrd1*$^{+/+}$ and *Nrd1*$^{-/-}$ mice were fed the CSAA or CDAA diets. Histology and oil red O staining showed that fat accumulation in the livers of both *Nrd1*$^{+/+}$ and *Nrd1*$^{-/-}$ mice occurred during administration of the CDAA or CSAA diets and increased in a time-dependent manner, although fat accumulation in *Nrd1*$^{+/+}$ mice was more prominent than that in *Nrd1*$^{-/-}$ mice (Figure 1A). Size of fat deposition was greater in *Nrd1*$^{+/+}$ mice than in *Nrd1*$^{-/-}$ mice in both diet groups at each time point (Figure 1A), and triglyceride levels in the liver were significantly higher in *Nrd1*$^{+/+}$ mice (Figure 1B). There was no significant difference in the liver/body weight ratio between *Nrd1*$^{+/+}$ and *Nrd1*$^{-/-}$ mice fed CSAA or CDAA diets (Figure 1C). Thus, administration of CSAA or CDAA diets induced hepatic steatosis in mice to a varying degree. However, serum ALT levels were significantly increased in *Nrd1*$^{+/+}$ mice upon administration of the CDAA diet, whereas they were not increased in *Nrd1*$^{-/-}$ mice fed the CDAA diet (Figure 2A). Serum ALT level was elevated in neither *Nrd1*$^{+/+}$ nor *Nrd1*$^{-/-}$ mice fed the CSAA diet (Figure 2A). Consistent with these findings, qRT-PCR showed that mRNA expression of inflammatory cytokines, such as IL6 and IL1-β, was significantly increased only in *Nrd1*$^{+/+}$ mice fed the CDAA diet when fat accumulation and elevation of ALT were prominent, whereas they were not increased in *Nrd1*$^{-/-}$ mice fed the CDAA diet, and in both *Nrd1*$^{+/+}$ and *Nrd1*$^{-/-}$ mice fed the CSAA diet (Figure 2B). These data indicated that nardilysin played an important role in the development of steatohepatitis and accompanied the production of inflammatory cytokines in mice fed the CDAA diet.

Nrd1 was required for sufficient secretion of TNF-α

TNF-α is one of the key molecules that are involved in the development of NASH [4–7,20]. Because secretion of activated TNF-α is the initial step in nardilysin-mediated production of inflammatory cytokines [12], we hypothesized that sufficient secretion of TNF-α by nardilysin is required for the development of steatohepatitis. Thus, we aimed to ascertain whether TNF-α was produced and secreted sufficiently in the livers of *Nrd1*$^{+/+}$ and *Nrd1*$^{-/-}$ mice fed the CDAA diet. qRT-PCR showed that the mRNA of TNF-α was increased in both *Nrd1*$^{+/+}$ and *Nrd1*$^{-/-}$ mice fed the CDAA diet, and that in contrast to the results looking at IL6 and IL1-β mRNA levels, there was no significant difference between *Nrd1*$^{+/+}$ and *Nrd1*$^{-/-}$ mice (Figure 2B). Immunohistochemistry showed that TNF-α protein was detected in F4/80-positive Kupffer cells or macrophages in both *Nrd1*$^{+/+}$ and *Nrd1*$^{-/-}$ mice fed the CDAA diet for 20 weeks (Figure 3A, right, arrowheads). Conversely, TNF-α protein was barely detected in F4/80-positive Kupffer cells or macrophages in both *Nrd1*$^{+/+}$ and *Nrd1*$^{-/-}$ mice fed the control CSAA diet for 20 weeks (Figure 3A, left). The number of F4/80-positive cells/×100 high power field (HPF) in the liver was slightly increased only in *Nrd1*$^{+/+}$ mice fed the CDAA diet but not in *Nrd1*$^{-/-}$ mice fed the CDAA diet and those